How closely can a solid approach an air-water surface without becoming wet?

F. P. A. Cortat and S. J. Miklavcic
Department of Science and Technology, Linköping University, Campus Norrköping, S-601 74 Norrköping, Sweden
(Received 4 April 2003; revised manuscript received 16 July 2003; published 20 November 2003)

Through a study of the van der Waals interaction between a solid and an air-water interface, we investigate the practical and fundamental problem of the limiting height at which an object can approach a free surface. A numerical study of the interface shape reveals dependencies governed by two disparate length scales associated with the relative strengths of the van der Waals and bouyancy forces, to surface tension. A study of the limits of solvability of the governing equation has led to the principal result: a closed-form expression for the absolute limiting height to which an object can be lowered to the air-water interface. The formula depends explicitly and only on the Hamaker constant of the van der Waals force and the geometry of the solid.

DOI: 10.1103/PhysRevE.68.052601 PACS number(s): 68.03.Cd, 68.03.Hj

Imagine a child playing beside a pool of water, testing to see how close he can place his finger to the water surface. He is instinctively aware that he cannot come too close, for the surface will spontaneously jump to meet his approaching finger. In laboratory studies, researchers use the sensitive Wilhelmy plate technique to measure surface properties of the pure air-water interface, or properties of an air-water interface containing a precise selection of surface active molecules [1,2]. The experiment involves the edge-on immersion of a metal plate, suspended by a fine wire from a force sensor, into the water. In doing so, the researcher notices that no matter how slowly and carefully she lowers the plate toward the water surface, it does not meet a placid horizontal surface.

In both instances the water surface does not remain flat during the object's descent. Instead, being fluid and hence deformable, the interface responds to the presence of a solid body. Invariably, the water surface becomes subject to an induced stress—*a surface force*. In the given solid-air-water system, the imposed stress, a van der Waals interaction, is attractive depending explicitly on a parameter A, called the Hamaker constant, and the locations of the two surfaces. The van der Waals attraction causes the water surface to bulge in the direction of the solid. The extent to which it bulges depends on separation. A limiting, stable bulge corresponding to a limiting approach distance is inevitable.

Appearing now for the first time, to our knowledge, are explicit formulas for the limiting height a solid can be lowered toward the air-water surface. Exact calculations of limiting stable water surface profiles are summarized in simple formulas involving elementary functions. The formulas are applicable to a wide range of macroscopic objects and can be utilized by experimentalists and laymen alike. These results are based on accepted approaches already adopted in related studies [3–8].

To understand what happens at and to the water surface as a solid is lowered toward the interface, we perform a theoretical study by modeling the object as a smooth body of cylindrical symmetry. Specifically, the solid is represented by a cylindrical coordinate pair $(r,z_p(r))$ where z_p is a smooth function. The corresponding air-water interface is represented by the coordinate pair $(r,z(r))$, in which the function $z=z(r)$ must be determined.

For simplicity the solid body considered is a cylindrical paraboloid whose profile in vertical cross-section is described by the function $z_p(r)=z_{p0}+\lambda r_p^2$. The value z_{p0} denotes the lowest-most point of the paraboloid cylinder, while the shape of the body is governed by the *splay* parameter λ, $r_p=r_p(r)$ where r is the sole independent coordinate variable. Typical z_{p0} values of relevance are of the order of a few hundred to a few thousand nanometers, approximately 10 000–100 000 times smaller than the horizontal scale. By varying λ, which plays a central role in the forthcoming analysis, we can effectively model any shape of parabolic solid from a planar interface ($\lambda\to 0$) to a vertical line ($\lambda\to\infty$). The larger the value of λ, the sharper or more needlelike the solid is.

The van der Waals surface energy,

$$\sigma(r,z(r),z_p(r))=-\frac{A}{2D(r,z(r),z_p(r))^2}, \tag{1}$$

resulting from a summation of intermolecular interactions depends explicitly on the locations of both surfaces through the distance function $D(r,z(r),z_p(r))$, connecting points on the two surfaces by the shortest line segment (see Fig. 1). The Hamaker constant A is a measure of the strength of the intermolecular interactions, and thus a function of the three materials involved [9]. In all σ is a function of the paraboloid shape and material properties, i.e., $\sigma=\sigma(r,z(r);A,z_{p0},\lambda)$. WIth the fluid media presumed of infinite depth, the complication of involving similar interactions between either the fluid surface or the paraboloid and an underlying solid substrate [5] can be avoided.

The shape of the water surface, $(r,z(r))$, is determined via an Euler-Lagrange minimization of the total free energy of the system [11,8]. The Euler-Lagrange equation satisfied by $z(r)$ is [8]

$$\frac{d}{dr}\left\{\frac{rz_r(r)}{W(r)}[\gamma+\sigma(r,z,z_p)]\right\}=rW(r)\sigma_z(r,z,z_p)+rGz(r). \tag{2}$$

Here, partial derivatives with respect to independent variables r and z are denoted by subscripts; $W(r)=\sqrt{1+z_r^2}$ is an area scaling factor; and $G=\Delta\rho g$ is the product of the density

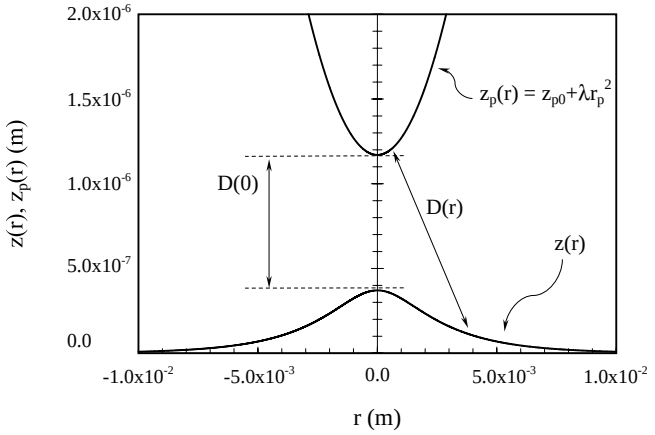

FIG. 1. Vertical cross section of a paraboloid $z_p(r)=z_{p0}+\lambda r_p(r)^2$, where $z_{p0}=1170$ nm while splay parameter $\lambda=0.1\ \mathrm{m}^{-1}$, and an air-water surface, $z(r)$. The water profile is a solution to Eq. (2) for a van der Waals interaction between the surfaces [10]. Physical parameters are: $z_{p0}=2020$ nm, splay parameter $\lambda=0.1\ \mathrm{m}^{-1}$, $\Delta\rho=0.9969\ \mathrm{g\,m/cm}^3$, $\gamma=72.8$ mN/m, and Hamaker constant $A=10^{-20}$ J. The figure also indicates the distance function $D(r,z(r),z_p(r))$.

difference between water and air, multiplied by the gravitational acceleration. The right-hand side of Eq. (2) contains a surface term associated with the induced van der Waals surface stress and a body force term arising from the gravitational contribution. These act in opposition. The former acts to lift the water surface above its neutral position ($z=0$) and is countered by the latter force, which is proportional to the relative mass of water raised. On the left-hand side of Eq. (2) appears a surface energy $\gamma+\sigma$, which measures the surface's ability to reduce the extent of deformation. Since σ is negative this ability is diminished compared to the bare surface, measured by the air-water surface tension γ.

Two principal length scales appear in this problem: one associated with the relative strength of the gravitational force to surface tension, $l_G=\sqrt{\gamma/G}$, the capillary length, and one, l_V, a complex function of z_{p0}, λ, as well as a length scale associated with the relative strength of the van der Waals stress to surface tension, $l_A=\sqrt{A/\gamma}$. Not surprisingly, the existence of these two length scales leads to profile shapes which differ in scale in the two orthogonal directions.

Full numerical solution of the Euler-Lagrange equation, Eq. (2), is achieved self-consistently and involves a matching of near- and far-field solutions. For details and complementary results see Ref. [10].

Solutions of Eq. (2) for a range of parameter values are typically represented by the profile in Fig. 1 which highlights the disparity between the vertical scale, $\sim l_V$, and the horizontal scale, $\sim l_G$. The figure includes both a calculated air-water interface profile (lower curve) and the solid paraboloid (upper curve) responsible for the van der Waals surface force. A recurring feature of solutions to Eq. (2) is that despite the local nature of the van der Waals stress ($\sim l_A$) the effect on the air-water interface extends some distance away from the apex of the pin, although this would not necessarily be apparent to the naked eye as, in contrast, the change in the surface elevation is only of the order of hundreds to at most thousands of nanometers. The prolonged influence on the profile follows the asymptotic behavior of the solution to Eq. (2),

$$z(r)\sim C\frac{\exp(-r/l_G)}{\sqrt{r}} \quad \text{as} \quad r\to\infty, \tag{3}$$

valid far from the region of closest approach of the solid. The rate at which the surface deformation diminishes depends on the decay length l_G which, for the air-water interface, is ≈ 0.27 cm. Consequently, a plane air-water interface whose lateral extent exceeds $10l_G$ or more can in this context be considered effectively infinite.

A solution of Eq. (2) is, however, not always possible. This fact plays a crucial role in determining how close an object can be placed to a water surface. If placed too close, then certain conditions necessary to ensure a solution to Eq. (2) will not be satisfied. The physical implication for an object too close to the water surface is that the water will preferably wet the solid. The solvability limit we speak of represents an *absolute* lower bound for the distance at which the solid can approach the air-water surface.

We have performed extensive numerical calculations of this limit of solvability, translated into a minimum height $z_{p0,\min}$ to which an object can be lowered toward a water surface. Obviously, this minimum height, $z_{p0,\min}$, is a function of both the Hamaker constant A and the paraboloid splay parameter, λ, as well as the surface tension of water γ and the gravitational force constant G. As focus here is on the air-water interface, no functional dependence on either γ or G can be deduced. In Fig. 2 we show examples of numerically determined, minimum limiting values of z_{p0}. These curves demonstrate quite a typical behavior as a function of either splay parameter or Hamaker constant, respectively. In each of the figures in Fig. 2, we also show the corresponding maximum height of the air-water interface which occurs at the apex, $z(0)$, i.e., directly under the paraboloid tip.

It seems reasonable that as the solid becomes broader and flatter (decreasing λ) the limiting height of approach (and thus limiting separation between solid and fluid) increases, since an increasing proportion of the solid comes within the van der Waals range of influence of the water interface. Similarily, the dependence on Hamaker constant is as follows: the greater the strength of the interaction (increasing A), the greater the minimum limiting height to which the body can come to the surface. Naturally, the limiting value of the peak in the air-water profile, $z(0)$, follows the trend in the $z_{p0,\min}$ values. Interestingly enough, there is a consistent factor of about 3 between corresponding limiting values of $z_{p0,\min}$ and $z(0)$.

For the numerical data presented in Fig. 2, showing dependence of $z_{p0,\min}$ on λ for a fixed Hamaker constant, we obtain a least squares fit of the form

$$z_{p0,\min}(\lambda;A=2\times10^{-19}\ \mathrm{J})=10^{\beta(\lambda)}\ \mathrm{m} \tag{4}$$

with exponent values $\beta=-5.7306-0.2036\log_{10}\lambda-0.0345(\log_{10}\lambda)^2$. On the other hand, with regard to the

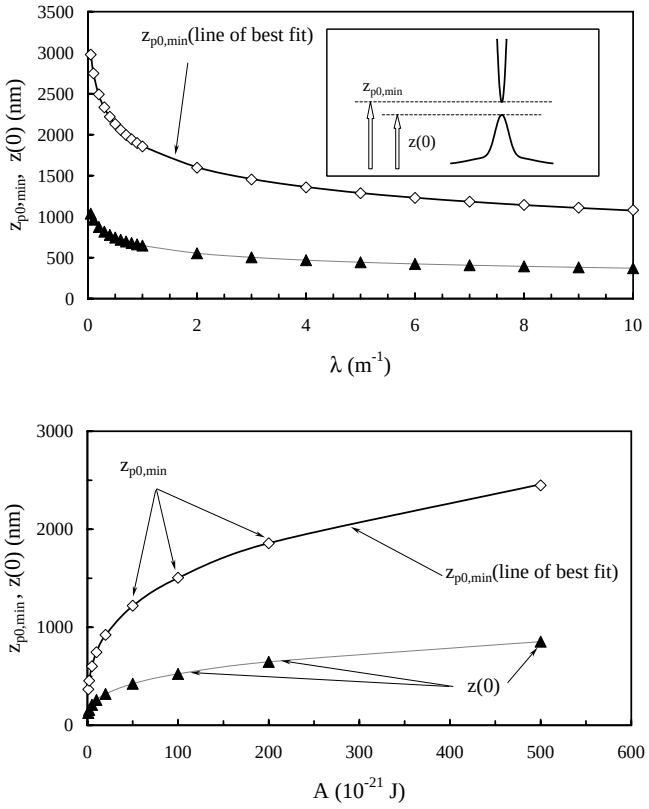

FIG. 2. Critical limiting heights $z_{p0,\min}$ (open diamonds) above a plane water surface ($z=0$) for a parabolic solid of cross section, $z_p(r)=z_{p0}+\lambda r_p(r)^2$, as a function of splay parameter λ, (upper figure) and Hamaker constant A (lower figure). Solid triangles show corresponding maximum heights of air-water interface. Solid curves are least squares fits to the $z_{p0,\min}$ values: $z_{p0,\min}=10^{-5.7306-0.2036\log_{10}\lambda-0.0345(\log_{10}\lambda)^2}$ (least squares fit, upper figure) and $z_{p0,\min}=10^{-6.4343}\times A^{0.3057}$ (least squares fit, lower figure). Physical parameter values: $\Delta\rho=0.9969$ gm/cm^3, $\gamma=72.8$ mN/m, and fixed Hamaker constant $A=2\times10^{-19}$J (upper figure) and fixed splay parameter $\lambda=1$ m^{-1} (lower figure).

dependence on A for fixed splay parameter, a least-squares analysis gives a best fit of the form

$$z_{p0,\min}(A;\lambda=1\ \mathrm{m}^{-1})=10^{\alpha}A^{\mu}\ \mathrm{m}, \tag{5}$$

where $\alpha=-6.4343$ and $\mu=0.3057$. These power-law fits are motivated by plots of the data on a log-log scale. Clearly, the exponent in Eq. (4) is specific to the value of A (and G and γ), while those in Eq. (5) are specific to the given value of λ (and G and γ). On the other hand, Eqs. (4) and (5) represent the same two-dimensional function of A and λ (for fixed G and γ). To determine this function, values of both A and λ spanning two orders of magnitude or more were studied. Specifically, we considered the range of Hamaker constants from 10^{-21} J to 5×10^{-19} J, and splay values λ from 0.05 m^{-1} to 10 m^{-1}. Values of λ less than 0.05 m^{-1} were difficult to implement. For $\lambda<0.05$ m^{-1} numerical problems arise because the paraboloid is too flat and an inherent system instability predominates. In the limit $\lambda\to0$ one has the inherently unstable system of an infinite solid plane interacting with an infinite fluid surface [3,5]. For $\lambda>10$ m^{-1} no immediate numerical difficulty arises. However, numerical calculations require a finer discretization of the r variable with a consequent increase in computation time. In contrast, no difficulty appears in the case of smaller values of A. While limits expected for A values are larger than those considered here, such are not typically found in practice.

From the assumption that the parameter dependence of $z_{p0,\min}$ is of form (5) and by varying $\lambda\in[0.05,10]$, we have deduced that

$$\alpha=-6.4341-0.2379\log_{10}\lambda-0.0236(\log_{10}\lambda)^2 \tag{6}$$

to a relative accuracy of 0.1%, while a more complex dependence on $\log_{10}\lambda$ applies for the second exponent. To third order we find the least-squares approximation

$$\mu=0.3057+0.014\,45\log_{10}\lambda-0.004\,385(\log_{10}\lambda)^2 -0.000\,022\,6(\log_{10}\lambda)^3+O((\log_{10}\lambda)^4) \tag{7}$$

in which the $O((\log_{10}\lambda)^4)$ term is positive and non-negligible. Motivated by experience with a related system involving a smaller density difference [10], we found that Eq. (7) could be rewritten approximately as

$$\mu\approx0.3057+[1-(3/10)\log_{10}\lambda+(3/10)^2(\log_{10}\lambda)^2 -(3/10)^3(\log_{10}\lambda)^3+\cdots][0.01445\log_{10}\lambda-1.3252\times10^{-3}(\log_{10}\lambda)^3] \tag{8}$$

in which we recognize the expression within the central parentheses as the first few nontrivial terms of the binomial expansion for $(1+x)^{-1}=\Sigma_{n=0}^{\infty}(-1)^n x^n$ for $|x|<1$. Anticipating that successive terms continue to follow the binomial series the implied summation was performed to give, for $|\log_{10}\lambda|<10/3$, the approximation

$$\mu\approx0.3057+[0.1445-1.3252\times10^{-2}(\log_{10}\lambda)^2]\frac{\log_{10}\lambda}{10+3\log_{10}\lambda} \tag{9}$$

to the "exact" least-squares formula, Eq. (7). Equation (9) intrinsically possesses all orders of contributions of $\log_{10}\lambda$ and thus better represents the λ dependence.

Invoking Eq. (6) in Eq. (5), with μ given by Eq. (9), we obtain the convenient, closed-form formula

$$z_{p0,\min}=10^{-6.4341}\lambda^{-0.2379-0.0236\log_{10}\lambda}A^{\mu}\ \mathrm{m} \tag{10}$$

for the critical minimum height of a macroscopic object above the air-water interface. This formula depends only on the type of material making up the solid (Hamaker constant) and its geometrical curvature (splay parameter).

Formula (10) reproduces the numerically determined $z_{p0,\min}$ values over the given $A\lambda$-parameter space to an accuracy of less than 2% relative error for the two lowest λ values: $\lambda=0.05$ and 0.1 m^{-1} and less than 0.5% relative error for the remainder. The error decreases as λ increases up to $\lambda=10$ m^{-1}.

It is important to note that in Eq. (4)–(10) λ and A must be normalized with respect to the reference scales $\lambda_{ref}=1\ \mathrm{m}^{-1}$ and $A_{ref}=10^{-21}$ J, respectively. Use of any other system of units will lead to error. The critical height expressed by Eq. (10) is given in meters.

Once immersed and withdrawn from the water, the stability limit given originally by Eq. (10) will no longer apply due to the additional thin water film on the surface of the wet solid. Depending on film thickness, the operative Hamaker constant for this four-layer system may be quite different. If thick enough, the appropriate Hamaker constant would be that for the water-air-water configuration. This is generally the most attractive case of any triple layer system involving water and an intervening air medium [9]. With an increased Hamaker constant, the wet solid would not be able to come as close to the water surface as when dry, all other things being equal.

The limiting height formula, Eq. (10), based on the geometric assumption of a paraboloid solid cylinder, has wider applicability than first supposed. By invoking the so-called Derjaguin approximation [12], applicable to short range surface forces, the limiting height formula, Eq. (10), could be used with any smooth convex macroscopic body provided that the splay constant λ be chosen appropriate to the solid's mean curvature at the point of closest approach (e.g., a sphere against a flat surface).

Even with the Derjaguin approximation use of Eq. (10) is valid for macroscopic solids only. For specialized applications in experiments quantifying the mesoscopic interaction between microscopic or submacroscopic solids and various fluid surfaces [13–22], an accurate representation requires fitting of exact numerical calculations in the range $\lambda=100$–$10\,000\ \mathrm{m}^{-1}$. Here, an accurate fitting formula obtained in a similar fashion to Eq. (10) turns out to be (for $\lambda\in[100,10\,000]$)

$$z_{p0,\min}\approx 10^{-6.4341}\lambda^{-0.2579-0.0071\log_{10}\lambda}A^{\mu}\quad \mathrm{m}, \tag{11}$$

with

$$\mu\approx 0.3057+0.039\,\frac{\log_{10}\lambda}{3+\log_{10}\lambda}. \tag{12}$$

Again, the fitting agrees extremely well with the calculated limiting approach distances; a relative error of less than 1.0% for $\lambda\geqslant 100\ \mathrm{m}^{-1}$, often better. Thus, given the maximum height of an isolated sessile drop above a fixed reference level (say supporting substrate) in a typical atomic force microscope experiment, Eq. (11) can be used to determine the minimum possible substrate-colloidal particle separation.

So, how closely can a solid approach an air-water surface without being wet? Equations (10) and (11) answer this question by allowing one to calculate in ideal situations the *absolute* minimum height one can lower an object.

[1] G.L. Gaines, *Insoluble Monolayers at Liquid-Gas Interfaces* (Wiley Science, New York, 1966).
[2] F. MacRitchie, *Chemistry at Interfaces* (Academic Press, New York, 1990).
[3] S. Churaev, A. Starov, and B.Y. Derjaguin, J. Colloid Interface Sci. **89**, 16 (1982).
[4] M. Forcada, M.M. Jakas, and A. Grasmati, J. Chem. Phys. **95**, 706 (1991).
[5] M. Forcada, J. Chem. Phys. **98**, 638 (1993).
[6] S.J. Miklavcic, R.G. Horn, and D.J. Bachmann, J. Phys. Chem. **99**, 16 357 (1995).
[7] D.Y.C. Chan, R.R. Dagastine, and L.R. White, J. Colloid Interface Sci. **236**, 141 (2001).
[8] S.J. Miklavcic and P. Attard, J. Phys. A **34**, 7849 (2001).
[9] J.N. Israelachvili, *Intermolecular and Surface Forces*, 2nd ed. (Academic Press, New York, 1992).
[10] F.P.A. Cortat and S.J. Miklavcic (unpublished).
[11] R. Courant and D. Hilbert, *Methods of Mathematical Physics* (Wiley, New York, 1965), Vol. 1.
[12] B.V. Derjaguin, Kolloid-Z. **69**, 155 (1934).
[13] W.A. Ducker, Z. Xu, and J.N. Israelachvili, Langmuir **10**, 3279 (1994).
[14] H.-J. Butt, J. Colloid Interface Sci. **166**, 109 (1994).
[15] M.L. Fielden, R.A. Hayes, and J. Ralston, Langmuir **12**, 3721 (1996).
[16] R.G. Horn, D.J. Bachmann, J.N. Connor, and S.J. Miklavcic, J. Phys.: Condens. Matter **8**, 9483 (1996).
[17] S. Basu and M.M. Sharma, J. Colloid Interface Sci. **181**, 443 (1996).
[18] P.G. Hartley, F. Grieser, P. Mulvaney, and G.W. Stevens, Langmuir **15**, 7282 (1999).
[19] D.E. Aston and J.C. Berg, J. Colloid Interface Sci. **235**, 162 (2001).
[20] D. Bhatt, J. Newman, and C.J. Radke, Langmuir **17**, 116 (2001).
[21] P. Attard and S.J. Miklavcic, J. Colloid Interface Sci. **247**, 255 (2002).
[22] S.A. Nespolo, D.Y.C. Chan, F. Grieser, P.G. Hartley, and G.W. Stevens, Langmuir **19**, 2124 (2003).